Journal of Engineering for Gas Turbines and Power, Volume 136, Issue 9, September 2014, Article number 091201
DOI: 10.1115/1.4027216

Impact of Inlet Filter Pressure Loss on Single and Two-Spool Gas Turbine Engines for Different Control Modes

Uyioghosa Igie and Orlando Minervino

Energy and Power Division

Cranfield University,

Bedfordshire, MK43 0AL, UK

email: u.igie@cranfield.ac.uk

tel: +44 (0) 1234 758382

ABSTRACT

Inlet filtration systems are designed to protect industrial gas turbines from air borne particles and foreign objects, thereby by improving the quality of air for combustion and reducing component fouling. Filtration systems are of varying grades and capture efficiencies, with the higher efficiency systems filters providing better protection but higher pressure losses.

For the first time, two gas turbine engine models of different configuration and capacities have been investigated for two modes of operation (constant TET and load/power), for a 2 and 3-stage filter system. The main purpose of this is to present an account on factors that could decide the selection of filtration systems by gas turbine operators, solely based on performance.

The result demonstrates that the two-spool engine is only slightly more sensitive to intake pressure loss relative to the single-spool. This is attributed to higher pressure ratio of the two-spool, as well as the deceleration of the HPC/HPT shaft rotational speed in a constant TET operation. The compressor of the single-spool engine and the LPC of the two-spool shows similar behaviour: slight increase in pressure ratio and reduced surge margin at their constant rotational speed operation. Loss in shaft power is observed for both engines, about 2.5% at 1,000 Pa loss. For constant power operation there is an increase in fuel flow and TET and as a result the creep life was estimated. The result obtained indicates earlier operating hours to failure for the 3-stage system over the 2-stage by only few thousand hours. However this excludes any degradation due to fouling that is expected to be more significant in the 2-stage system.

Keywords: gas turbine inlet filtration, pressure loss, single and two-spool and control modes

INTRODUCTION

Industrial gas turbine engines are fitted with inlet filtration system upstream of the gas turbine compressor intake to mainly mitigate blade fouling, erosion, corrosion and eradicate Foreign Object Damage (FOD). This aims to improve the quality of air through the engine gas path. Typically particles above 10 μm can cause blade erosion [1,2], while particles below this size often cause blade fouling [3,4]. Good filtration system comes with lots of advantages and often unquantifiable benefits, however the downside is the pressure loss induced on the gas turbine associated with better capture efficiency. High Efficiency Particulate Air (HEPA) filters with superior capture efficiency are to be designed to remove 99.97% of particles of 0.3 μm as set by the United States Department of Energy (DOE-STD-3020-2005). Schroth and Cagna [5] reports a capture efficiency of 98.9% for particles ranging between 0.3 to 0.5 μm when a 3-stage (F6-F9-H11 filter arrangement) system is employed.

Figure 1 indicates the placement of inlet filtration system, fitted upstream of the gas turbine compressor intake. For some installations a by-pass door is in place to avoid very high differential pressure across the filter. This is typical in very cold climates, desert environment during sandstorm and a very humid condition for which the self-cleaning filters rapidly become loaded. Filter media are of different types however filters are classed according to their capture efficiency or arrestance as shown on Table 1. This table adapted from Wilcox et al. [1] and Turnbull et al. [6] indicates that the highest grade filters can capture very fine particles below 0.01 μm. Their capture efficiency is defined as the ratio of the number or volume of particles captured in the filter to the particles entering the filter, multiplied by 100. The ASHRAE and EN standards indicated are based on dry duct laboratory test which may differ from that obtained in operation on site [6]. Wilcox et al. [7] demonstrates a preliminary validation study indicating the changes in filter performance in wet conditions. Further reading on the respective ASHRAE and EN standards is available in open literature.

It is important to state that the best performance occurs when the filters become loaded with particles and not at the start of their useful lives. There would also be an increase in pressure loss over time, as the filters become loaded with particles. Different filter systems have different starting or initial pressure drop. In some environments the filter would be quickly loaded therefore leading to higher pressure drops and earlier replacement of filters. However in such environment, the potential damaged that could have occurred without these filters can be more expensive. On the other-hand, a far less polluted environment may not require the best performance filters as they may never reach the maximum quoted efficiency before replacement [1]. These points out the importance of identifying the appropriate filter type for a given environment/site.

The focus of this study is to investigate the impact of filter inlet pressure drop for static staged filter, which consist of a number of number of filter stages for which the stage capture efficiency increases progressively. The initial stage filter (pre-filter) usually captures larger particles while the last stage would capture finer particles. The initial stage filters could be replaced during engine operation; however the last stage filter is normally changed during shut-down of the engine [2]. Figure 2 depicts an example of a filter arrangement adapted from Wilcox et al. [1]. This as shown consists of the following:

A. **Weather hood:** to reduce mainly water and some moisture from gaining access to the filter system. They are applied in most filter system installation especially in environments with high amount of rainfall and snow or ice (tropical, costal/off-shore and winter conditions). This therefore protects the filter systems from too much wetting that can weaken the filter media structure and increase pressure drop [8,9].
B. **Trash or Insect Screen (Primary filters):** mainly captures or deflects insects, leaves and other objects, therefore ensuring that the filters do not become quickly overloaded with particles.
C. **Coalescer (Primary filters):** to reduce high liquid moisture, especially in off-shore, costal and marine environments. Meher-Homji and Bromley [9] indicates that under high ambient humidity conditions, many filters unload salt, leading to sudden increase in compressor fouling. Coalescers are very useful in collecting small droplets of liquid which can contain salt aerosols that is difficult to eliminate using other filter media type. The small droplets are collected on the filter media, forming bigger droplets that are trapped from the main flow.
D. **Pre-filters**: could be bag type as indicated in Fig. 2, the rectangular/panel type or an inertial separator that is more effective for larger particle capture/separation. The first two filters types mentioned could be made with glass fibre or synthetic media while the other works mainly on the basis of particle inertia and the centrifugal effect of an axial swirl generator that throws the particles radially towards the casing of tube. These mentioned pre-filters are typically of a class F9 and below using Table 1.
E. **HEPA filter:** indicated here is a rectangular type. These filters are characteristically between class H10 and H14 and are currently the highest grade filters for gas turbine and turbomachinery applications. The self-cleaning or pulse filters is another HEPA type filter commonly applied in

environments with high dust particle concentration, where the filters become loaded quickly, such as desert environment. They are characterised by the additional self-cleaning at certain level of pressure drop. The operation of the self-cleaning filter is achieved by a brief back-pulse of air extracted from the gas turbine compressor section or an auxiliary source [8]. The pulse air pressure is between 5.5 to 7 bar pressure, within 100 to 200 ms, occurring only 10% of the elements for any given time [10]. However the downside of this is the penalty on gas turbine performance or the additional cost of an auxiliary unit.

It is common to have filter systems classified as 2 or 3-stage arrangements. An example is Schroth and Cagna [5] that presents a study with emphasis on comparing the 2 and 3-stage systems (F6-F8 and F6-F9-F11 sequence respectively). Taylor [11] provides an operator's view based on several filter arrangements including the G3-F4-F8, G3-F6-F9 and G3-F5-E11 sequence without any reference to number of stages. It should be noted that though some studies categorize filter systems based on stages, there is currently no strict convention yet. Nevertheless a filter arrangement with a least one F-Class type and no H-Class type of filter is often a 2-stage system. Conversely, an arrangement with a H-Class is regarded as 3-stage. This type of filter would always come after an F-Class pre-filter that captures bigger particles, therefore extending its use, and for all cases of arrangement, a G-Class filter comes first to capture the biggest particles.

The main aim of this study, unlike any study available in open literature, is to demonstrate the impact of inlet pressure drop on single and two-spool engines, for different engine control modes using a 2 and 3-stage filter system. Subsequent section starts with the description of engine models and code implemented, thereafter the case of filter loss investigated from actual engine data and then the outcomes.

SIMULATION CODE AND ENGINE MODELS

The performance of a single and two-spool engine has been modelled and simulated using TURBOMATCH, a Cranfield University in-house program written in FORTRAN. The zero-dimensional steady-

state computer program simulates the design and off-design performance of most gas turbine configurations using a modified Newton-Raphson method as the convergence technique. This simulation code consists of standard compressor and turbine maps that allows for map scaling and combustion temperature rise chart embedded in the program. Design point calculation is carried out with initial user specification of ambient conditions, pressure losses, component efficiencies, etc. as shown subsequently. Convergence is achieved in the component matching after satisfying compatibility of non-dimensional rotational speed and flow between the compressor and turbine. The off-design compressor and turbine component operating point on their maps are determined based on their calculated scaling factors indicated in Eq. (1) to (8). An iterative procedure is employed and it involves several trials to ensure that the variables are consistent with the matching constraint (e.g. fixed Turbine Entry Temperature –TET).

The Compressor

For off-design calculation, the scaling equations applied to obtain the scaling factors for the compressor is as follows

$$PRSF = \frac{PR_{Dp} - 1}{PR_{Map.Dp} - 1} \tag{1}$$

$$WASF = \frac{WAC_{Dp}}{WAC_{Map.Dp}} \tag{2}$$

$$ETASF = \frac{\eta_{C\,Dp}}{\eta_{C\,Map.Dp}} \tag{3}$$

Subscript *Dp* is the specified new design point value and *Map.Dp* is the design point value on the standard map. The scaling factors are also used to generate the new compressor maps. For the compressor, the measure of the proximity to the surge line known as the compressor surge margin is also specified and it is defined by Eq. (4).

$$SM = \frac{PR_{Dp} - PR_{HIGH}}{PR_{HIGH} - PR_{LOW}} \tag{4}$$

The Turbine

For the turbine component driving the compressor, the flow function (also known as the swallowing coefficient) scaling factor is

$$TFSF = \frac{TF_{Dp}}{TF_{Actual}} \tag{5}$$

That of the shaft speed scaling factor is

$$CNSF = \frac{CN_{Dp}}{PCN} \tag{6}$$

PCN is the shaft speed in % and CN is the non-dimensional speed

$$CN = \frac{PCN}{\sqrt{TA}} \tag{7}$$

The scaling factor of the work function is

$$DHSF = \frac{DH_{Dp}}{DH_{Map}} \tag{8}$$

And the turbine efficiency scaling factor is the same formula indicated in Eq. (3), but relating to the turbine.

The Combustor

The combustor efficiency is a plot of combustion efficiency and temperature rise for different constant inlet pressure. This is defined as

$$\eta_{Comb} = \frac{ideal\ amount\ of\ \ fuel\ burnt}{actual\ amount\ of\ \ fuel\ burnt} \tag{9}$$

A schematic of the engine considered in this investigation is indicated in Figs. 3 and 4. The single-spool has the same shaft connecting the compressor, turbine and a generator (that converts auxiliary shaft power to electrical power) as depicted. The two-spool configuration is slightly different in the anatomy, with an additional shorter shaft wound around the longer LPC/LPT shaft as shown. The rotational speed for the two-spool HPC/HPT shaft is variable. This study focuses on gas turbine application for power generation, and hence the shaft connected to the assumed generator is rotating at a constant speed for both models. The models do not consist of a generator however the generator work is the net power. (i.e. turbine work – compressor work).

The design point specified parameters for both engine models are indicated in Table 2. As observed, the single-spool engine has a greater shaft power (MW) than the two-spool engine, however the pressure ratio of the latter is higher as a result of the HP spool ability to rotate at a higher speed compared to the LP spool. Both engine model specifications are inspired by the Siemens V94.3A and General Electric LM6000 engines and as such, comparable design point parameters obtained from public domain at ISA conditions have been used in this study. The bottom of the table indicates the parameters obtained from design point calculation.

INLET FILTRATION PRESSURE LOSS CASE

The case of inlet filter pressure loss investigated is indicated in Fig 5. Measurements were taken every 1 hour from the 1st day of the month to the last day, the 30th. This adds up to be 720 hours (721 data points) during

this period. As would be observed, the pressure loss at 0 hours is around 400Pa or 4mbar. This is not the starting pressure loss for this 2-stage filter system, but rather the start of measurements taken and provided. Filter systems can have an initial total pressure loss starting from 200 – 400 Pa, depending on the filter types, class and media in use. Figure 5 shows that pressure loss increases to 700 Pa and it is attributed to the environmental contaminants build-up. This proceeds to the period of filter cleaning, reducing the pressure loss to about 300 Pa at 326 hours. The pressure drop plot isn't smooth. This is a result of the contributing effects of temporarily increased concentration of contaminants, effects of relative humidity or even fluctuating volume flow rate of the GT as explained in Schroth and Cagna [5].

The filter pressure losses over this month are implanted into both engine models as off-design cases. In addition to this, a 3-stage arrangement is investigated by simplistically increasing the pressure losses at every given hour by 300 Pa. This difference is recommended by Schroth and Cagna [4] based on their observed measured average pressure drops for engines installed with 2-stage system and 3-stage systems from operational experience. Figure 6 shows that the highest pressure loss for the assumed 3-stage system is 1,000 Pa. This differential pressure is approximately the maximum allowable final pressure loss a gas turbine filters is made to operate. Wilcox and Brun [12] indicates this for a 2-stage system, as well as Taylor [11] for a 3-stage system. It is important to reiterate that that reaching very high pressure loss is dependent on the level of environmental contamination and rate of loading on filter systems. The concept of a 3-stage system adopted here from Schroth and Cagna [4] is to differentiate two systems for which in the case of the 3-stage, more particles would be trapped as a result of the fineness of the filter systems, as well as an additional stage, usually H-Class for better protection.

IMPACT ON GT ENGINE PERFORMANCE

This off-design behaviour has been simulated for two control modes: constant temperature and constant load for both engines.

Temperature Control (Constant TET)

In this operation the TET is fixed and maintained every given time. It is common to run gas turbine engines in this mode especially for combined cycle, where a given EGT is required to extract a given power from the steam turbines. When operating close to the maximum capacity of the engine, this control option is used to keep away from the TET/EGT due to concerns about the turbine blade creep life.

From Fig. 7 for the single-spool, it can be observed that generally the power output is the same until about 70 hours when then there is an incremental pressure loss and then there is a noticeable drop in power output. This is mainly due to constrained flow capacity reduction associated with particle build up in the filter housing. This persists till 350 hours when the pre-filter was replaced. These can be summarised into three periods, which individually shows similar power outputs. The reason for these flat lines is as a result of lower sensitivity to small changes in pressure drop. Bigger changes in pressure loss around 100 Pa bring about more noticeable changes to the engine performance. This is also indicated in Fig. 8 that shows the percentage power output loss associated with pressure loss relative to a clean case. These Figs. show that for the 2-stage system the power output is higher due to the lower pressure loss. As a result the thermal efficiency indicated in Fig. 9 for the 2-stage system is better at every given time.

This appears to be an advantage for the 2-stage system, however in practical terms more amounts of particles would have access into the gas turbine engine, fouling the compressor and also leading to further reduced performance.

For brevity, similar trends for the two-spool is not included, nevertheless Table 3 summarises the loss in power output in 720 hours for both engines for the two filtration systems. The table shows smaller accumulative loss in power output in the 2-stage system. The loss in the single-spool engine is about 5 times greater than the two-spool. This is mainly due to the higher rating of the single-spool engine which also has an inlet mass flow that is 5 times that of the two-spool. A more appropriate comparison is in terms of % change as illustrated in Fig. 10. This shows that the two-spool engine is slightly more sensitive to fouling than the single-spool. The reason for this is that the two-spool has a higher pressure ratio and a second spool that reduces its rotational speed in this control mode due to pressure loss. This is best illustrated using the compressor maps however the changes are very small to show and hence presented in Table 4. This indicates the impact of 1,000 Pa (maximum loss in the month) on both engines. For the single-spool compressor the mass flow reduction at a constant rotational speed causes

the pressure ratio to increase, therefore reducing the surge margin. The two-spool LPC responds similarly, however the HPC rotational speed drops, reducing its pressure ratio and consequently increasing the HPC surge margin. In design terms, the extent of this depends on the stage loading of the LPC relative to the HPC. In this study the LPC has a pressure ratio of 2.45 while the HPC is 12.3.

Load Control (Constant Shaft Power)

For this control mode, the engine is governed to maintain the power output at all time. The changes in intake pressure losses indicated in Fig. 6 doesn't reduce or change the power output of the engine, as fuel is increased to accommodate for this. As a result the TET increases. This is indicated in Fig. 11 for the case of the single-spool. As observed, the TET increase in the case of the 3-stage system is higher due to higher filter losses. The highest rise in TET is 1,510 K which is about 10 K rise from the design clean engine. Figure 12 indicates the change in TET relative to the design engine for both engines applying 2 and 3-stage systems.

The respective additional fuel consumption for both engines, 2 and 3-stage systems for the month is presented in Table 5 and the percentage increase for the period on Fig. 13 shows that on average, the two-spool has slightly more fuel consumption about 0.2% difference (3-stage), which isn't significant. Its respective cases of 2 and 3-stage system for a given engine show just around 0.1% difference, which again isn't much.

IMPACT ON FIRST STAGE ROTOR BLADE LIFE

The Larson-Miller Time –Temperature Parameter approach has been applied to evaluate the first rotor blade creep life due to TET increase when the filter system becomes loaded with dust as discussed in the previous section regarding operation at constant power output. The Larson-Miller approach is based on the assumption

that an increase in the turbine blade operating temperature will reduce the time to reach a particular creep state. The expression is:

$$P = \frac{T}{1000}\left(\log_{10} t_f + C\right) \tag{10}$$

T is the rotor blade operating temperature, t_f is the time to failure and C is a material constant, given the value of 20 for industrial applications. To investigate this for the two-spool engine, the following assumptions have been made:

- Blade stress - the stress levels at the rotor blade of each individual engine is unchanged. This is because the parameters influencing stress levels on the blade do not change significantly, for the levels of pressure loss investigated here.
- A uniform metal temperature is assumed throughout the span and the chord of the blade.
- An average bulk gas temperature is assumed.
- A constant cooling effectiveness is assumed for the whole section of the blade. Advanced convection cooling is assumed.
- 1.9% of the total mass flow is allocated to blade cooling flow ϕ is assumed [13].
- Rene 5, which belongs to the family materials applied in aero and aeroderivative gas turbine HPT blades and it is considered in this study. Its application is highlighted in Walston et al. [14] and Hiroshi [15] with a P value of 29.6 which is around the working range of the material [14].

For this estimation, the HPT stage bulk gas temperature and HPC gas temperature were obtained from the engine model. The total mass flow for blade cooling flow ϕ is defined by Eq. (11).

$$\phi = \frac{m_c}{m_g} = m^* \frac{C_{p,g}}{C_{p,c}} St_g \frac{A_g}{A_b} \tag{11}$$

Where m_c is the coolant mass flow and m_g is the total engine mass flow. This can be substituted into the definition of the coolant mass flow function, m^*, which is the non-dimensional representation of the coolant's mass flow and can be rearranged into non-dimensional groups as

$$\frac{m^*}{\phi} = \frac{C_{p,c}}{C_{p,g}} \frac{1}{St_g} \frac{A_g}{N_b S_p L} \tag{12}$$

With $C_{p,c}/ C_{p,g}$ being the specific heat ratio of the coolant to the gas which is almost constant, $1/St_g$ representing the heat transfer coefficient can be assumed constant and Ag/N_bS_gL is a function of geometry which is constant. Consequently, as the individual terms are approximately constant they can be equal to a value K, hence the equation can be

$$m^* \approx \frac{\phi}{K} \tag{13}$$

With a constant K value, the relationship between the mass flow function and percentage of the engine's bleed cooling is linearly proportional and the value of K is around 2% to 3% for modern gas turbines [16]. A value of K = 2% is applied considering the technology of the engine considered. Using a chart of convective cooling efficiency, η_{co} versus cooling mass flow function, m^* for various cooling technique provided in Mukherjee [17] and Rubini [16] , the cooling effectiveness ε is obtained. The estimation of the rotor blade temperature was then achieved using Eq. (14), which is

$$T_{r.blade} = T_{b.gas} - \varepsilon \left(T_{b.gas} - T_{CDT} \right) \tag{14}$$

The HPT rotor blade temperature is subsequently calculated. The various TET, bulk gas temperature, CDT and corresponding duration are indicated in Table 6 which shows estimates applicable to the 2 and 3-stage operations. The 3-stage system has slightly higher rotor blade temperatures as expected, due to more increase in fuel flow indicated previously.

After the changes in the rotor blade temperature are derived, the time to fracture t_f is calculated using the Larson-Miller equation (Eq. (10)) for each individual set of rotor blade temperatures and the corresponding operating time

t at the specific temperature. The number of cycles to failure accumulatively can be estimated using Miner's rule mathematically expressed as:

$$\sum \frac{t}{t_f} \tag{15}$$

This is implemented and details are provided in Table 7 for the month. The number of hours to failure is also provided for the clean case of no filter pressure losses and that of the use of 2 and 3-stage systems. For the clean case, the operating hours to failure is 19,390 hours which is about 2.4 years, assuming 8,000 hours in a year. This estimate is comparable to that provided in Boyce [18], that shows the operation and maintenance life of industrial gas turbines for different applications and fuel type. The 2 and 3-stage filter systems in relation to the clean ideal case is short of 4,499 and 5,913 hours respectively, and the difference in hours to failure between both systems is 1,414 hours (about 2 months), excluding the potential impact of fouling, which will be more prevalent for the 2-stage system.

CONCLUSION

In summary, this investigation gives an account of the impact of inlet filter pressure loss on single and two-spool gas turbine engines, for varying control modes for 2 and 3-stage filter systems. The main conclusions are:

- Intake pressure loss can reduce power output up to 2.5% at high differential pressure of 1,000 Pa. Hence frequent changes of pre-filter can be beneficial especially in locations that are predisposed to severe particle contamination using static filters.
- The multi-spool gas turbine appears to be slightly more sensitive to intake losses. This is mainly due to the higher pressure ratio at which they operate and partly due to the deceleration of the HPC/HPT spool at constant TET operation. For constant power operation the HPC/HPT spool rotational speed increases due to increase in fuel flow. However this isn't sufficient to mitigate the penalty of high pressure loss.
- At constant TET, the difference in power loss in one month for the 2 engines individually, using 2 and 3 filters is really small comparatively. It should be noted that during operation, the 2-stage system relative to 3-stage system would allow for more particle penetration through the filters causing compressor fouling. This is not accounted for, and therefore suggests the possibility of further reduction in power output.
- For constant power operation the increased fuel flow and TET is highlighted. Again, the two-spool engine shows slightly higher sensitivity. For the case of pressure losses investigated, the engine has lost approximately 6 and 8 months of operating hours for the 2 and 3-stage systems respectively. Nevertheless, operating the engine without these systems in place could lead to unquantifiable loss; perhaps the whole machine in some extreme cases of surge induced by FOD. The inference to this study solely based on a performance view point, is that the 3-stage may still be the better alternative of the two options given the fact that the relative difference is small and the promise for better protection. It is also worth pointing that this study doesn't account for any possible online compressor washing that can be in place to clean/wash particles that gain access in to the engines, cost of filter systems and life of filter systems.

ACKNOWLEDGMENT

The authors owe gratitude and acknowledge Professor Pericles Pilidis of Cranfield University for his insightful advice and continuing support.

NOMENCLATURE

A_b	Cross sectional area of the blade, m^2
A_g	Cross sectional area of the blade that the bulk gas has an effect, m^2
C_p	Specific heat capacity at constant pressure, kJ/kg.K
C	Material constant
CN	Non-dimensional shaft speed relative to design
CNSF	Scaling factor for non-dimensional shaft speed

DH	Turbine work function
DHSF	Scaling factor of the work function
ETASF	Isentropic efficiency scaling factor
K	Cooling model parameter relates mass flow function and engine bleed cooling, %
L	Blade span, m
m*	Mass flow function of the coolant
MF	Mass flow of compressor, kg/s
MW·h	Megawatt hour - energy
N_b	Number of cooling channels per blade
P	Larson-Miller parameter
PCN	Shaft rotational speed as a percentage of design point, %
PR	Pressure ratio
PR_{HIGH}	Highest pressure ratio for a given constant speed line, at surge
PR_{LOW}	Lowest pressure ratio for a given constant speed line, at choke
PRSF	Pressure ratio scaling factor
S_p	Blade perimeterof the coolant channels of the blade, m
S_{tg}	Stanton Number of the gas
SM	Surge margin
t_f	Time to fracture, hours
t	Operating time at specific temperature, hours
T	Rotor blade operating temperature, temperature, K
$T_{b.gas}$	Bulk gas temperature, K
T_{CDT}	Compressor discharge temperature, K
$T_{r.blade}$	Rotor blade temperature, K
TA	Ambient temperature, K
TF	Turbine flow function or swallowing coefficient
TFSF	Scaling factor for turbine flow function using turbine map
WAC	Non-dimensional mass flow
WASF	Mass flow scaling factor
η_C	Compressor isentropic efficiency
η_{Co}	Convective cooling efficiency
η_{Comb}	Combustor efficiency

Greek Symbols

μm	Micrometer
ϕ	Blade cooling flow – the percentage of the engines bleed, %
ε	Convective cooling effectiveness

Subscripts

Actual	Value of quantity obtained from actual component conditions as opposed to map value
g	Gas
c	Coolant
Dp	Design point conditions
Map.Dp	Value of design parameter obtained from component map

Acronyms

ASHRAE	American society of heating, refrigerating and air conditioning engineers
CDT	Compressor delivery temperature, K
EGT	Exhaust gas temperature, K
EN	European
FOD	Foreign object damage
GT	Gas turbine

HEPA	High efficiency particulate air
HPC	High pressure compressor
HPT	High pressure turbine
ISA	International standard atmosphere
LPC	Low pressure compressor
LPT	Low pressure turbine
MW	Mega Watt
SS	Single shaft
TET	Turbine entry temperature, K
TS	Twin shaft

REFERENCES

[1] Wilcox, M., Baldwin, R., Garcia-Hernandez, A., and Brun, K., 2010, *Guideline for Gas Turbine Inlet Air Filtration Systems*, Gas Machinery Research Council, Dallas, TX.

[2] Hiner, S. D., 2011, "Strategy for Selecting Optimised Technologies for Gas Turbine Air Inlet Filtration Systems," ASME Paper No. GT2011-45225.

[3] Kurz, R., and Brun, K., 2012, "Fouling Mechanisms in Axial Compressors," J Eng Gas Turb Power, **134**(3), 032401.DOI:10.1115/1.4004403.

[4] Sawyer, J. W., 1972, Sawyer's Gas Turbine Engineering Handbook: Theory & design. Gas Turbine Publications, U.S.A.

[5] Schroth, T., and Cagna, M., 2008, "Economical Benefits of Highly Efficient Three-Stage Intake Air Filtration for Gas Turbines," ASME Paper No.GT2008-50280.

[6] Turnbull, G., Clément, E., and Ekberg, T., 2009, "Gas Turbine Combustion Air Filtration: Its Impact on Compressor Efficiency and Hot End Component Life," ETN Annual Workshop, Copenhagen, Denmark.

[7] Wilcox, M., Poerner, N., Kurz, R., and Brun, K., 2012, "Development of Test Procedure for Quantifying the Effects of Salt and Water on Gas Turbine Inlet Filtration," ASME Paper No. GT2012-69847.

[8] Loud, R. L., and Slaterpryce, A. A., 1991, "Gas Turbine Inlet Air Treatment," GE Power Generation, New York, U.S.A., GER-3419A.

[9] Meher-Homji, C., and Bromley, A., 2004, "Gas Turbine Axial Compressor Fouling and Washing," in 33rd Turbomachinery Symposium.

[10] Wilcox, M., Kurz, R., and Brun, K., 2011, "Successful Selection and Operation of Gas Turbine Inlet Filtration Systems," in 40th Turbomachinery Symposium.

[11] Taylor, S., 2012, "Implementing Improvements to Gas Turbine Air Inlet Filtration – An Operator Perspective," IDGTE Power Engineer, Vol. 16, no. 4, pp. 7-18.

[12] Wilcox, M., and Brun, K., 2011, "Gas Turbine Inlet Filtration System Life Cycle Cost Analysis," ASME Paper No. GT2011-46708.

[13] Eshati, S., 2012, "An Evaluation of Operation and Creep Study of a Stationary Gas Turbine," PhD Thesis, Cranfield University, U.K.

[14] Walston, W. S., O'Hara, K. S., Ross, E. W., Pollock, T. M., and Murphy, W.H., 1996, "RENE N6: Third Generation Single Crystal Superalloy," GE Aircraft Engines, Cincinnati, Ohio, U.S.A.

[15] Harada, H., 2003, "High Temperature Materials for Gas Turbines: The Present and Future," IGTC2003Tokyo KS-2.

[16] Rubini, P., 2012, "Turbine Blade Cooling," MSc Thermal Power Course notes, Cranfield University,U.K.

[17] Mukherjee, D. K., 1977, "Zur Schaufelkühlung der Gasturbine," Brown Boveri.

[18] Boyce, M., 2002, *Gas Turbine Engineering Handbook*, 2nd ed., Gulf Professional Publishing.

LIST OF FIGURES

LIST OF TABLES

Table 1: Grades of filter media, class and efficiency (ASHRAE and EU standards)

Grade	ASHRAE Class	EN Class	Arrestance (A) (%) Efficiency (E) (%)	Particles Separated
Coarse Dust Filter >10µm	1-4	G1	<65 (A)	Leaves, insects, textile fibres, sand, flying ash, mist, rain
		G2	65-80 (A)	
	5-9	G3	80-90 (A)	Pollen, fog, spray
		G4	>90 (A)	
Fine Dust Filter >1µm	10	F5	40-60 (E)	Spore, cement dust, dust sedimentation
	11-12	F6	60-80 (E)	Clouds, fog
	13	F7	80-90 (E)	Accumulated carbon black
	14-15	F8	90-95 (E)	Metal oxide smoke, oil smoke
		F9	95> (E)	
High Efficiency Particulate Air Filter (HEPA) >0.01µm	16	H10	85	Metal oxide smoke, carbon black, smog, mist, fumes
		H11	95	
	16	H12	99.5	Oil smoke in the initial stages, aerosol micro particles, radioactive aerosol
	17-18	H13	99.95	
	19-20	H14	99.995	Aerosol micro particles
Ultra Low Penetration Air Filter (ULPA)		U15	99.9995	Aerosol micro particles
		U16	99.99995	
		U17	99.999995	
Note: The correlation between the ASHRAE and EN standards classifications are approximates.				

Table 2: Engine model design point parameters

Specified Parameters	Single Spool	Two Spool
Specified Parameters		
Ambient condition	ISA – Sea Level	
Inlet Mass Flow	620 kg/s	127 kg/s
Intake Pressure Loss	1%	1%
Compressor Pressure Ratio	17	30
Compressor Efficiency	86%	88%
Combustor Efficiency	99%	99%
Combustor Pressure Loss	5%	7.5%
Turbine Efficiency	89%	89%
Turbine Entry Temperature	1,500 K	1,540 K
Shaft Power – Net Power	226 MW	40 MW
Calculated Parameters		
Fuel flow	14 kg/s	2.3 kg/s
Thermal Efficiency	37%	41%

Table 3: Accumulative loss in energy after 720 hours

Less Power×Hours (MW·h)	2-Stage System	3-Stage System
Single-Spool	3,305.03	4,040.10
Two-Spool	635.29	772.19

Table 4: % Δ in pressure ratio, surge margin, mass flow and rotational speed

	ΔMF (%)	ΔPCN (%)	ΔPR (%)	ΔSM (%)
SS Comp.	2.05 ▼	-	0.53 ▲	0.05 ▼
TS LPC	2.01 ▼	-	0.20 ▲	0.35 ▼
TS HPC	2.01 ▼	0.10 ▼	0.19 ▼	0.01 ▲

Table 5: Increase in fuel consumption for both engines

Increase in Fuel Consumption (kg)	2-Stage System	3-Stage System
Single-Spool	44.75	54.94
Two-Spool	10.05	12.09

Table 6: Inputs to calculate the rotor blade temperature for the two-spool engine

Two-Spool Engine				
2-Stage Filter System				
TET	Gas Bulk $T_{b.gas}$ (K)	Operating Hours	Compressor Discahrge T_{CDT} (K)	Rotor Blade $T_{r.blade}$ (K)
1,543.5	1,454	5	820	1,223.8
1,546.0	1,456	122	820	1,225.1
1,543.7	1,454	177	820	1,223.8
1,548.4	1,458	36	820	1,226.4
1,544.6	1,455	381	820	1,224.5
3-Stages Filter System				
TET	Gas Bulk $T_{b.gas}$ (K)	Operating Hours	Compressor Discahrge T_{CDT} (K)	Rotor Blade $T_{r.blade}$ (K)
1,546.8	1,457	2	820	1,225.7
1,547.7	1,458	380	820	1,226.4
1,548.1	1,458	54	820	1,226.4
1,549.6	1,459	249	821	1,227.0
1,551.5	1,461	36	821	1,228.6
Blade Cooling Parameters				
		m^*=0.95		
		n_{Co}=0.6		
		ε=0.36		

Table 7: Larson-Miler parameter life to failure analysis results for the two-spool engine

Two-Spool Engine				
Clean filters				
Operating Time (Hours)	Rotor Blade $T_{r.blade}$ (K)	P		t/tf
721	1,218.7	29.6	19,390	0.0372
Fraction of creep life used in one 721 h cycle				0.0372
Number of cycles to failure				26.9
Operating hours to failure				19,390
2-Stage filter system				
Operating Time (Hours)	Rotor Blade $T_{r.blade}$ (K)	P		t/tf
182	1,223.8	29.6	19,390	0.0118
381	1,224.5	29.6	14,925	0.0255
122	1,225.1	29.6	14,497	0.0084
36	1,226.4	29.6	13,686	0.0026
Fraction of creep life used in one 721 h cycle				0.0484
Number of cycles to failure				20.7
Operating hours to failure				14,891
3-Stage filter system				
Operating Time (Hours)	Rotor Blade $T_{r.blade}$ (K)	P		t/tf
2	1,225.7	29.6	14,089	0.0001
434	1,226.4	29.6	13,686	0.0317
249	1,227.0	29.6	13,295	0.0187
36	1,228.6	29.6	12,350	0.0029
Fraction of creep life used in one 721 h cycle				0.0535
Number of cycles to failure				18.7
Operating hours to failure				13,477

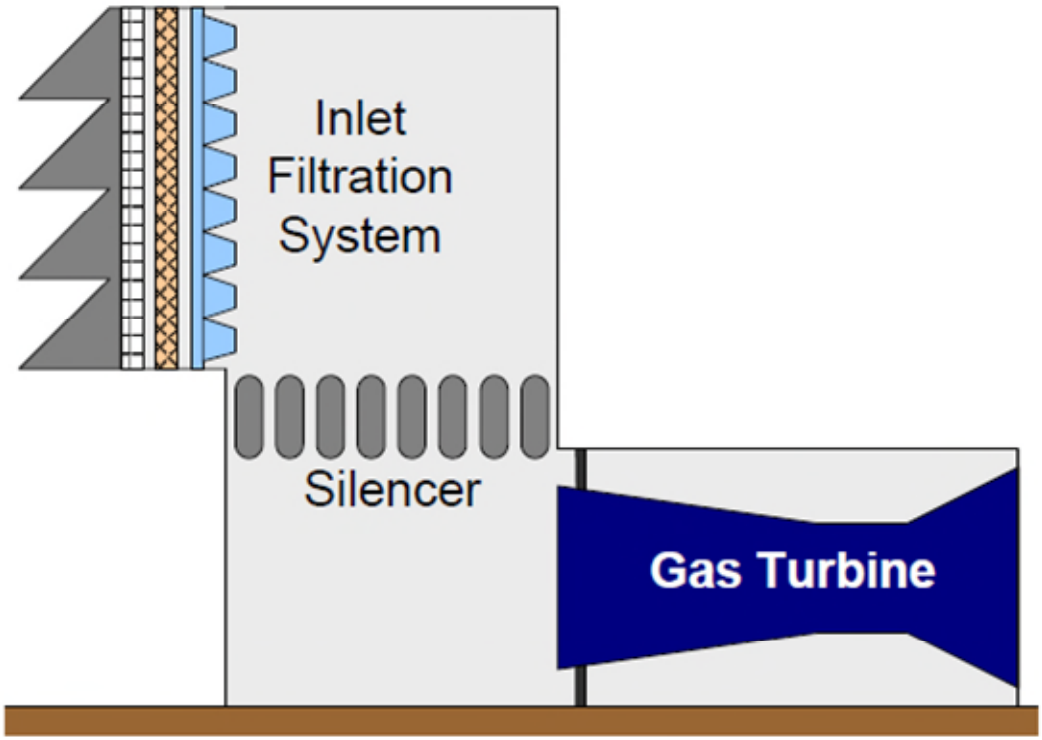

Fig1.tiff

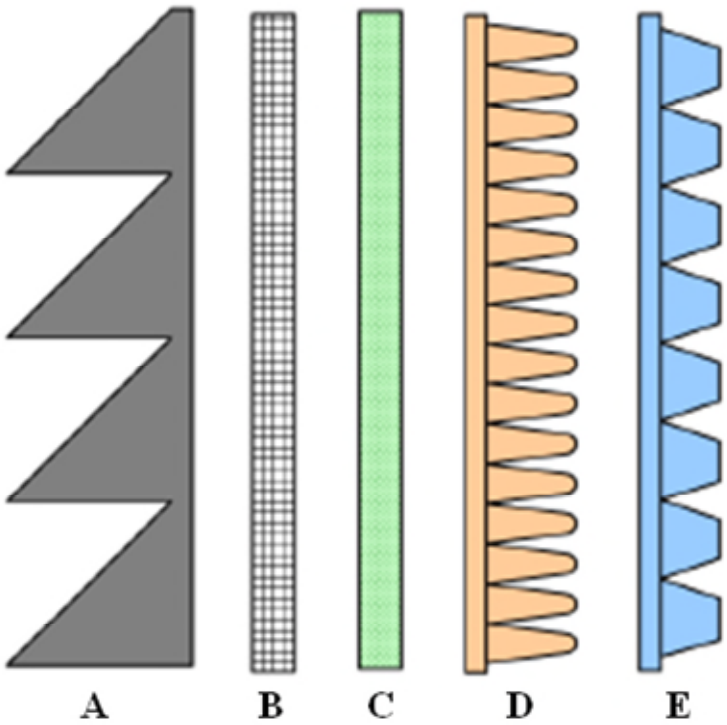

Fig2.tiff

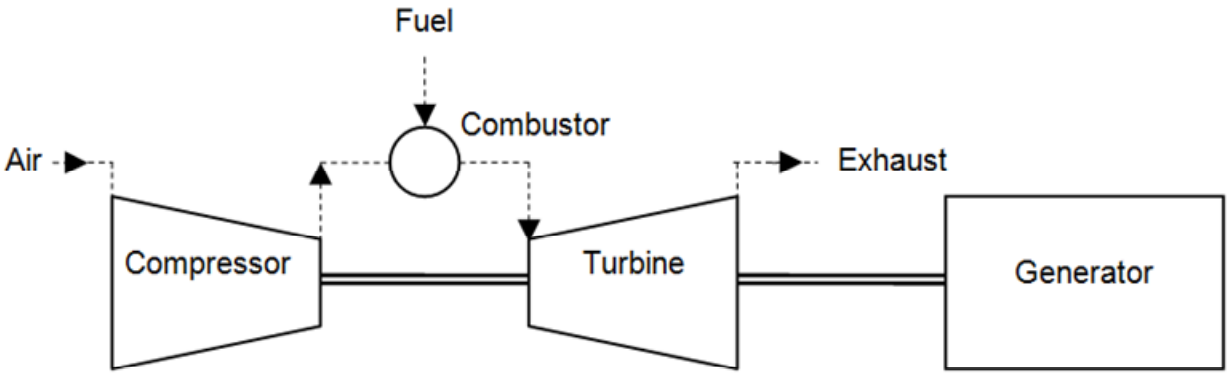

Fig3.tiff

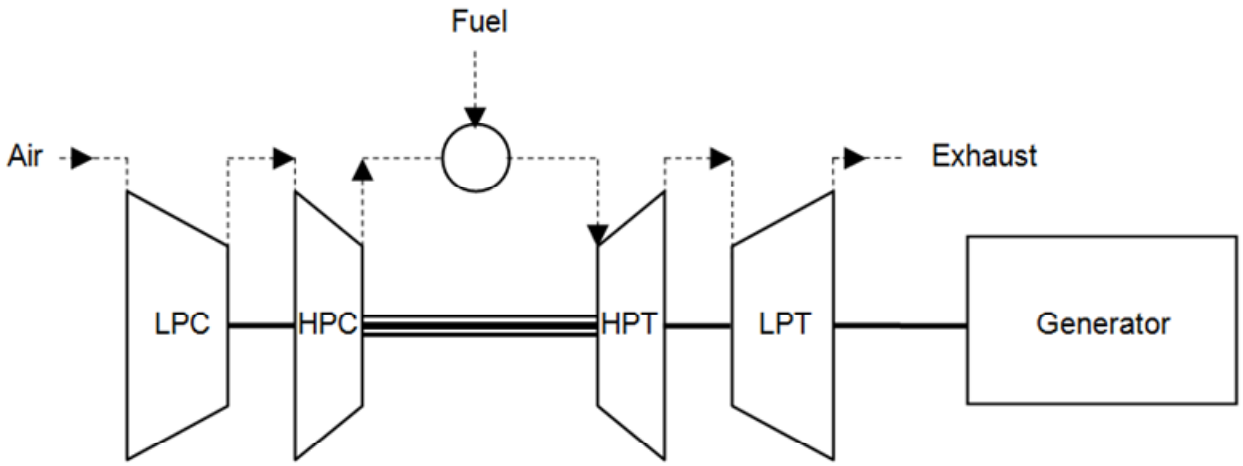

LPC/T – Low Pressure Compressor/Turbine

HPC/T – High Pressure Compressor/Turbine

Fig4.tiff

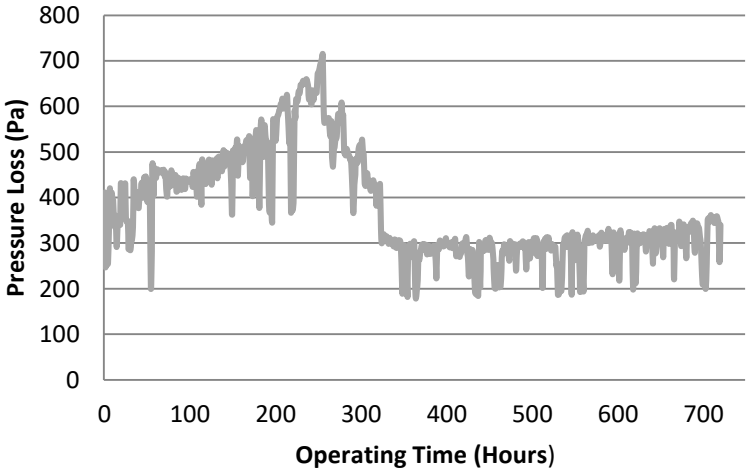
800
700
600
500
400
300
200
100
0
Pressure Loss (Pa)
0
100
200
300
400
500
600
700
Operating Time (Hours)

Fig5.tiff

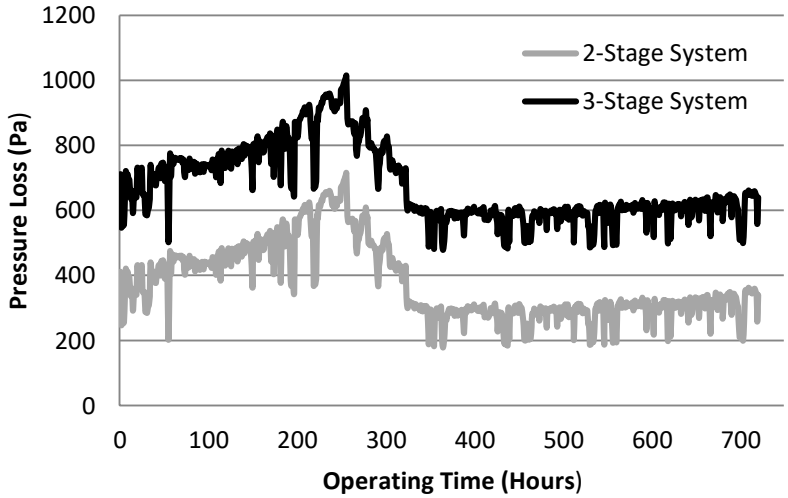
1200
1000
800
600
400
200
0
Pressure Loss (Pa)
0
100
200
300
400
500
600
700
Operating Time (Hours)
2-Stage System
3-Stage System

Fig6.tiff

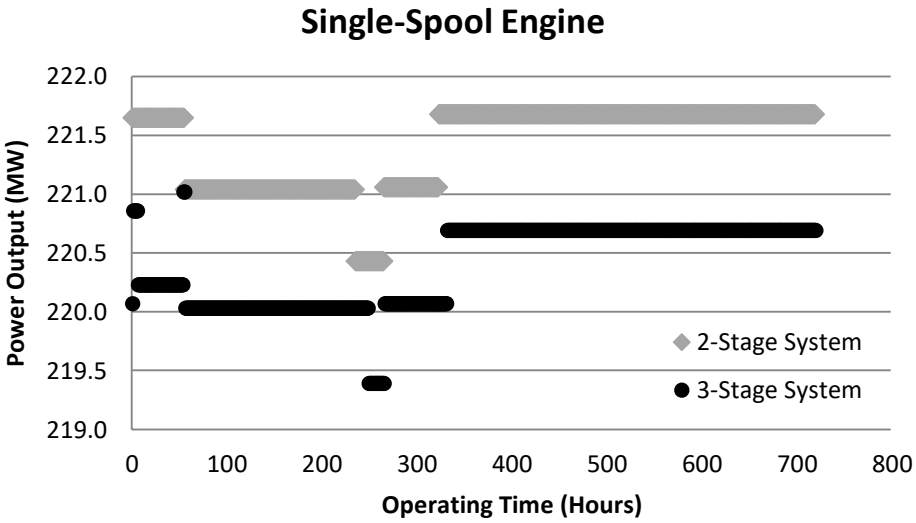
Single-Spool Engine
222.0
221.5
221.0
220.5
220.0
219.5
219.0
Power Output (MW)
0
100
200
300
400
500
600
700
800
Operating Time (Hours)
2-Stage System
3-Stage System

Fig7.tiff

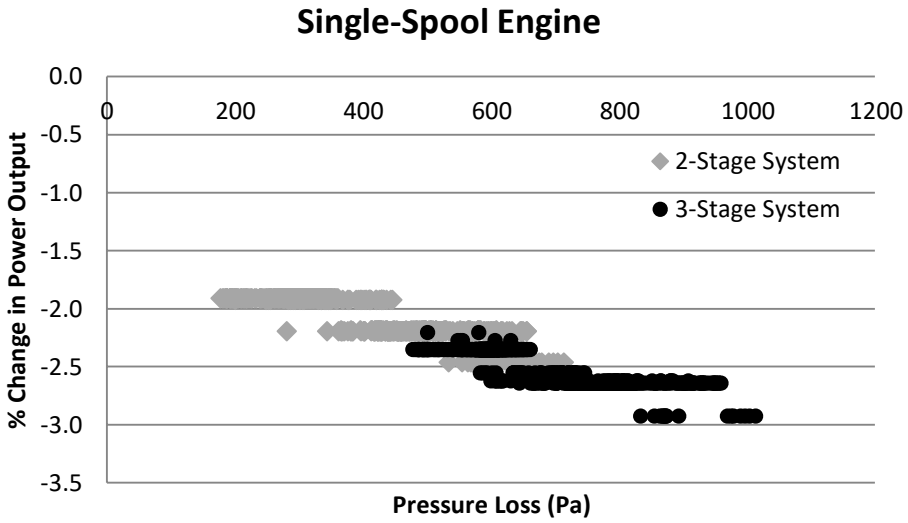
Single-Spool Engine
0.0
-0.5
-1.0
-1.5
-2.0
-2.5
-3.0
-3.5
0
200
400
600
800
1000
1200
% Change in Power Output
Pressure Loss (Pa)
2-Stage System
3-Stage System

Fig8.tiff

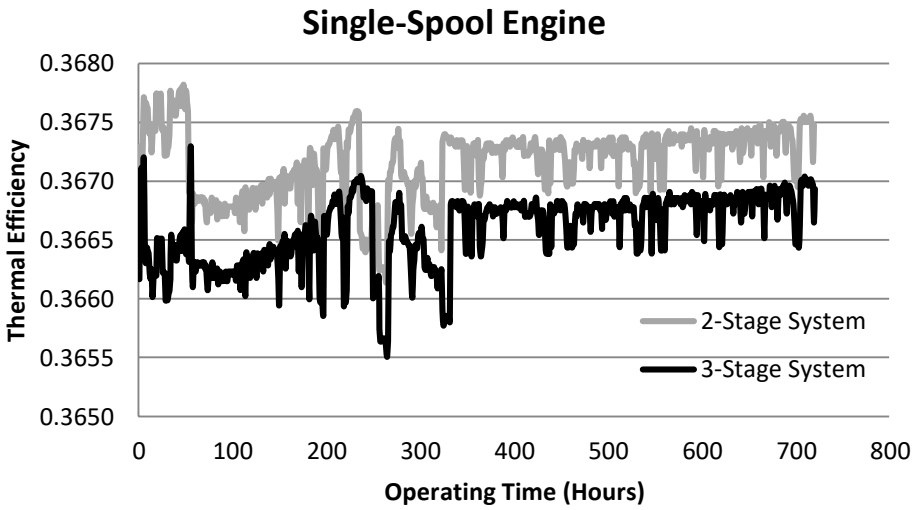
Single-Spool Engine
Thermal Efficiency
0.3680
0.3675
0.3670
0.3665
0.3660
0.3655
0.3650
0
100
200
300
400
500
600
700
800
Operating Time (Hours)
2-Stage System
3-Stage System

Fig9.tiff

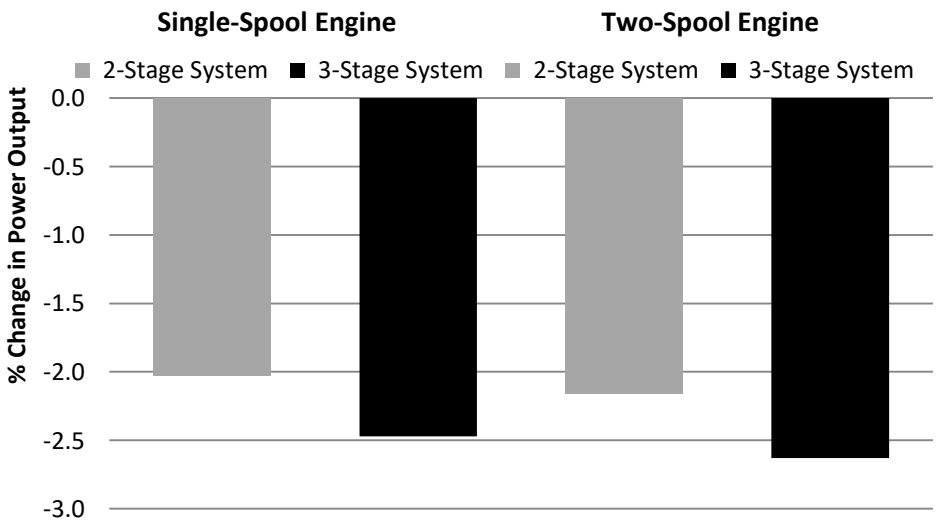
Single-Spool Engine
Two-Spool Engine
2-Stage System
3-Stage System
2-Stage System
3-Stage System
% Change in Power Output
0.0
-0.5
-1.0
-1.5
-2.0
-2.5
-3.0

Fig10.tiff

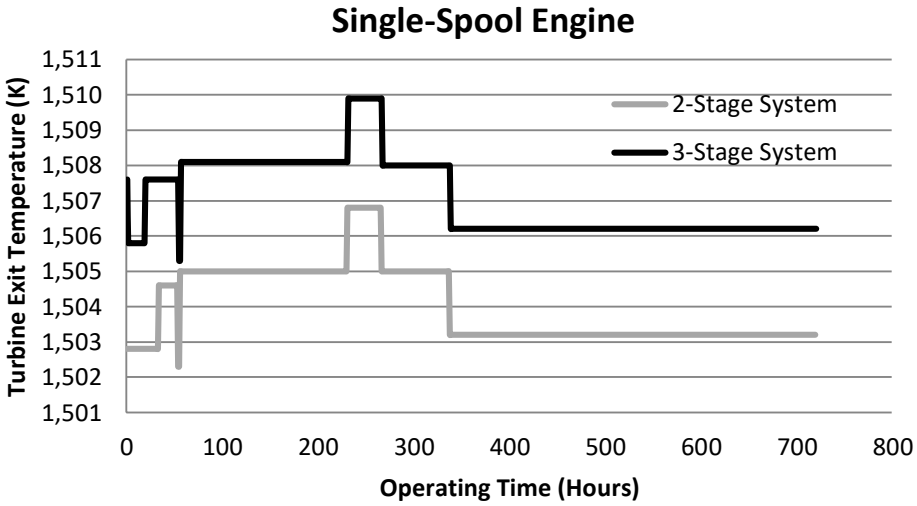
Single-Spool Engine
Turbine Exit Temperature (K)
1,511
1,510
1,509
1,508
1,507
1,506
1,505
1,504
1,503
1,502
1,501
0
100
200
300
400
500
600
700
800
Operating Time (Hours)
2-Stage System
3-Stage System

Fig11.tiff

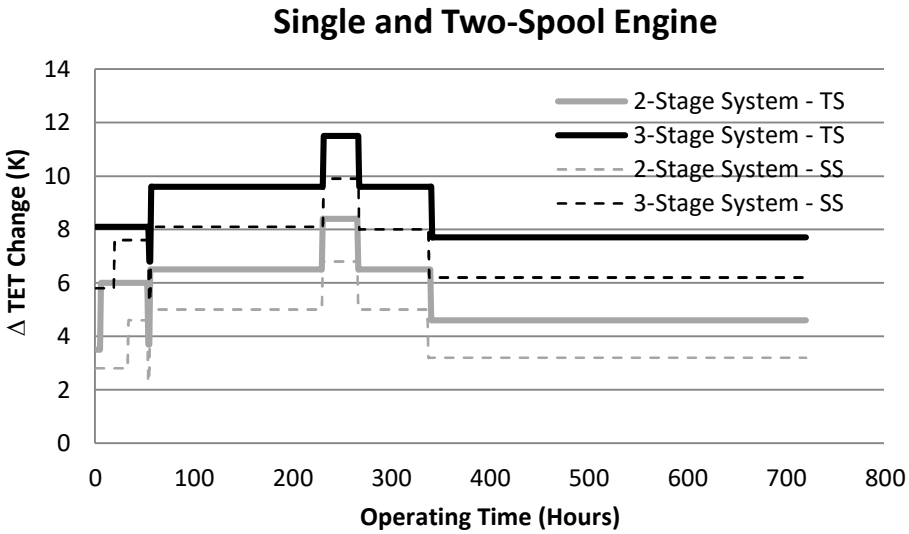
Single and Two-Spool Engine
14
12
10
8
6
4
2
0
Δ TET Change (K)
0
100
200
300
400
500
600
700
800
Operating Time (Hours)
2-Stage System - TS
3-Stage System - TS
2-Stage System - SS
3-Stage System - SS

Fig12.tiff

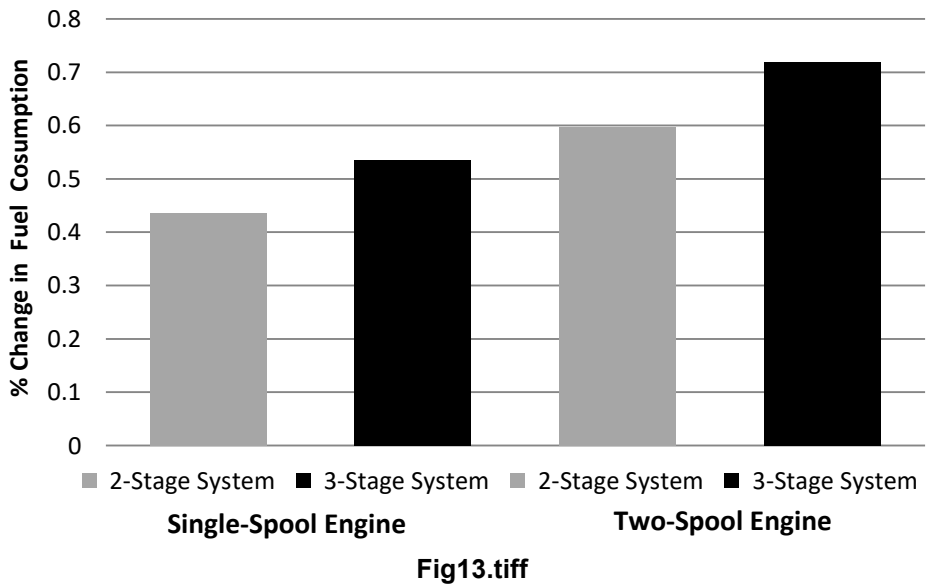
0.8
0.7
0.6
0.5
0.4
0.3
0.2
0.1
0
% Change in Fuel Cosumption
2-Stage System
3-Stage System
2-Stage System
3-Stage System
Single-Spool Engine
Two-Spool Engine

Fig13.tiff

Impact of inlet filter pressure loss on single and two-spool gas turbine engines for different control modes

Igie, Uyioghosa

2014-05-05

Igie U, Minervino O. (2014) Impact of inlet filter pressure loss on single and two-spool gas turbine engines for different control modes. Journal of Engineering for Gas Turbines and Power, Volume 136, Issue 9, September 2014, Article number 091201

https://doi.org/10.1115/1.4027216